

# A NEW BOOST DC-DC CONVERTER WITH A Y-Δ COMMUTATION CELL

Mauro Tavares Peraça and Ivo Barbi

Power Electronics Institute - INEP

Dept. of Electrical Engineering - EEL

Federal University of Santa Catarina – UFSC

P. O. box 5119 – 88040-970 – Florianópolis – SC- Brazil

peraca@inep.ufsc.br - ivobarbi@inep.ufsc.br

**Abstract** - This paper presents a new non-isolated step-up DC-DC converter, based on a commutation cell of three terminals and four switching stages which uses one high frequency three-phase transformer with a Y-Δ connection. The principle of operation of this converter is described and the main theoretical waveforms are shown, as well as the experimental results. The main expressions for the design of the converter and its output characteristic are also presented. This converter's advantages are: the frequency at the input and output filters is 3 times the switching frequency; a decrease in conduction losses; distribution of the currents without the need for control circuitry to balance them. Due to these characteristics, this converter is recommended for low voltage and high current applications.

**Keywords** – DC-DC converter, cell of three terminals, four stages cell.

## I. INTRODUCTION

The use of the classic boost converter in circuits with low voltage and high current inputs usually results in excessive losses; to minimize these losses, techniques that employ converter paralleling, such as *interleaving*, are generally used. Using this technique requires the addition of control circuits to balance the current among the converters, besides the use of several input inductors, one for each converter.

[1] and [3] present boost converters that operate with 2 switches associated with a transformer with a central tap; this topology presented good results, however it does not allow the use of a larger number of switches. On the other hand, in [2], a topology based on the Zig-Zag transformer is presented, which allows the use of 3 or more switches.

In this work, a new non-isolated boost converter based on a commutation cell that uses a high frequency three-phase Y-Δ transformer, as shown in Fig.1, will be presented. This converter presents the following advantages: it does not require control circuits to balance the currents; the frequency of the input and output filters is three times the switching frequency; the conduction losses are reduced. The Y-Δ switching cell can also be used with the other DC-DC converters.

With the main features of the proposed converter in mind, different applications such as power sources, telecommunications power sources, solar energy systems, fuel cells systems and fed by batteries systems can be listed.

The Y-Δ cell presents three operational regions, given as a function of the duty cycle, which are:  $0 < D < 1/3$ ,  $1/3 < D < 2/3$ ,

and  $2/3 < D < 1$ . Next, the characteristics of the boost converter for the  $D < 1/3$  operating region will be presented. The basic waveforms and the output characteristic of the remainder of the regions will be shown.

## II. OPERATING PRINCIPLES OF THE BOOST CONVERTER OPERATING AT $0 < D < 1/3$

It is assumed that the converter operates in steady-state, the switching frequency is constant, PWM is used, the components are ideal, and the turns ratio is equal to one. The drive signals of the switches are phase-shifted 120 degrees from each other.

### A. Continuous Conduction Mode - CCM

Next, the operation of the converter in continuous conduction mode is described. Fig. 2 illustrates the operational stages of the boost converter operating in CCM with  $D < 1/3$ . Fig. 3 presents the main waveforms of the converter for this operational mode.

#### 1<sup>st</sup> Stage ( $t_0 < t < t_1$ )

At  $t_0$ , switch S1 starts conducting and diode D1 is blocked. This operational stage is shown in Fig. 2a, where the branches through which the current flows are represented as thicker lines.

Due to the magnetic effect of the transformer, the currents of the three primary windings are identical, therefore, the current of the input inductor is divided into three, one part flowing through winding A1 and switch S1, and the others flowing through windings B1 and C1 and diodes D2 and D3, respectively.

Notice that the voltage applied across winding A1 during this stage is  $2/3$  of the output voltage. The equivalent circuit of this operational stage is presented in Fig. 4a and the voltage across the input inductor is given by equation (1).

$$V_L = V_{in} - \frac{2}{3}V_{out} \quad (1)$$

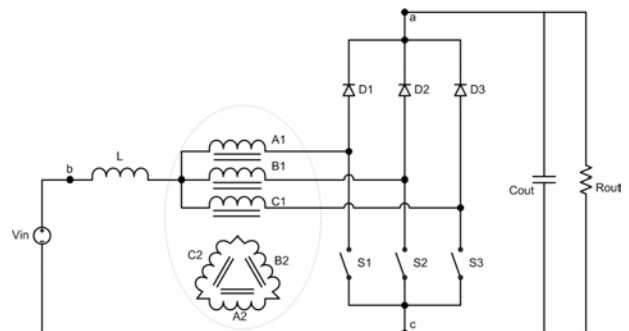


Fig. 1 – Boost Converter.

*2<sup>nd</sup> Stage ( $t_1 < t < t_2$ )*

At  $t_1$ , switch S1 is blocked, causing diode D1 to start conducting. Fig. 2b shows this operational stage.

Notice that the windings are short-circuited by the diodes, causing the voltage across them to be zero. The equivalent circuit of this operational stage is presented in Fig. 4b and the voltage across the input inductor is given by equation (2).

$$V_L = V_{in} - V_{out} \quad (2)$$

*3<sup>rd</sup> Stage ( $t_2 < t < t_3$ )*

At  $t_2$ , switch S2 starts conducting and diode D2 is blocked. Fig. 2c shows this operational stage. The behavior of the circuit during this operational stage is similar to the first stage, differing only in the switch that conducts.

*4<sup>th</sup> Stage ( $t_3 < t < t_4$ )*

At  $t_3$ , switch S2 is blocked, causing diode D2 to conduct. Fig. 2b shows the aforementioned operating stage, which is identical to the second stage, already described.

*5<sup>th</sup> Stage ( $t_4 < t < t_5$ )*

At  $t_4$ , switch S3 starts conducting and diode D3 is blocked. Fig. 2d shows this operational stage. Like the third stage, the behavior of the circuit during this stage is similar to the first stage.

*6<sup>th</sup> Stage ( $t_5 < t < t_6$ )*

At  $t_5$ , switch S3 is blocked, causing diode D3 to conduct. Fig. 2b shows this operational stage, which ends at  $t_6$  when switch S1 starts to conduct, beginning a new period.

*B. Static gain in CCM*

The converter's static gain can be obtained by the energy balance of the converter for each switching period. For this converter in particular, only 1/3 of the period needs be analyzed, since from the viewpoint of energy transfer, the stages repeat themselves every 1/3 of the period.

Equation (3) presents on one side of the equality the input energy and on the other side the output energy. Reorganizing equation (3), the static transfer characteristic in CCM is obtained. This result is given by equation (4) and shown in Fig. 5.

It's important to state that in CCM the proposed converter's static transfer characteristic is equal to that of the classic boost converter, independent of the operating region.

$$V_{in} \cdot I_L \cdot \frac{T}{3} = V_{out} \cdot \frac{2}{3} I_L \cdot D \cdot T + V_{out} \cdot I_L \cdot \left( \frac{1}{3} - D \right) \cdot T \quad (3)$$

$$\frac{V_{out}}{V_{in}} = \frac{1}{1-D} \quad (4)$$

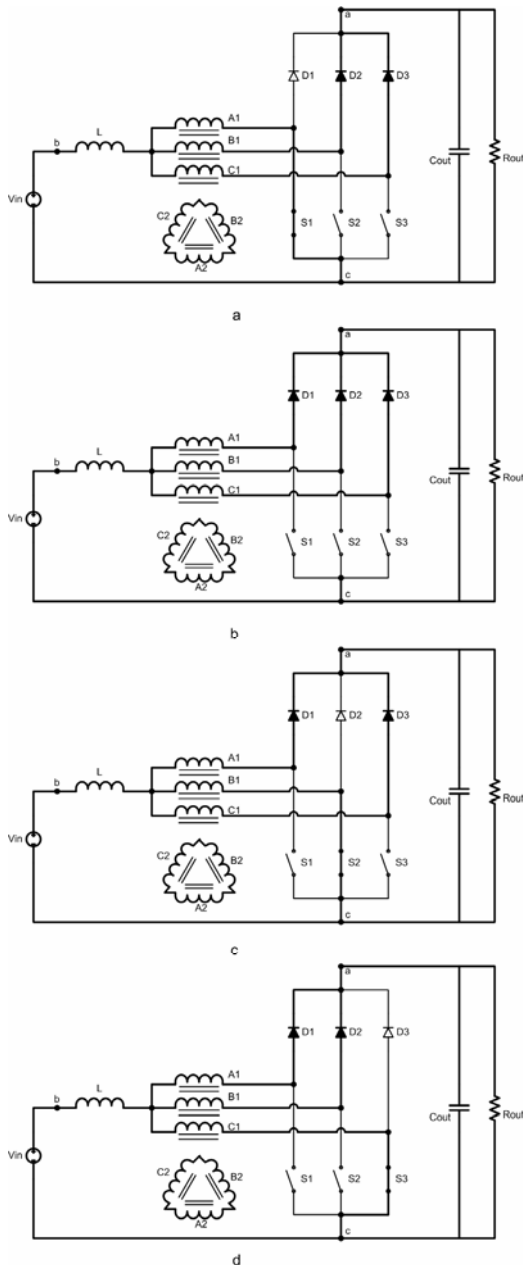


Fig. 2 – Operating stages in CCM.

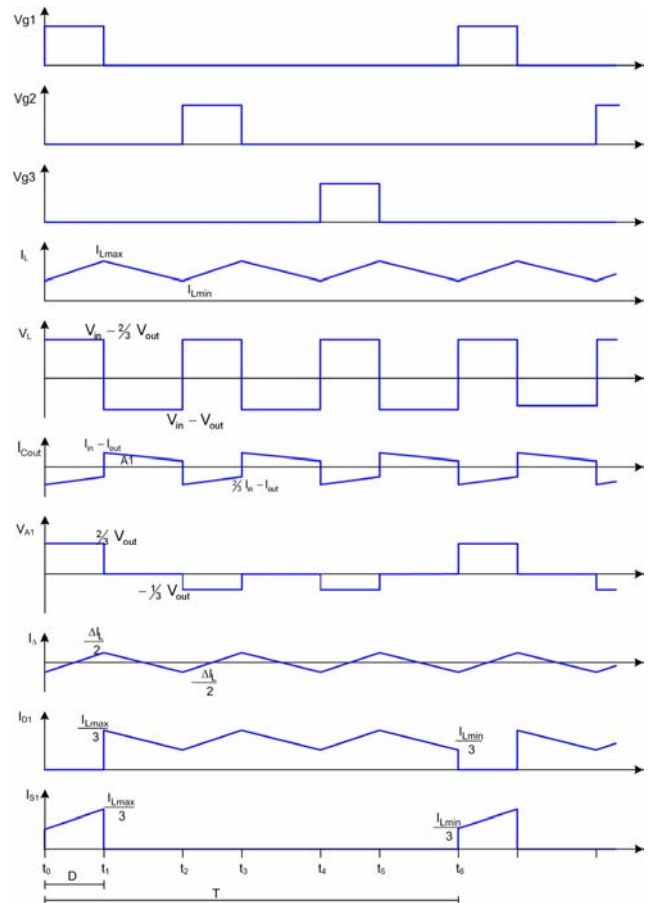


Fig. 3 – Basic waveforms in CCM. ( $D < 1/3$ )

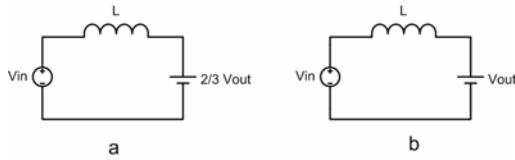


Fig. 4 – Equivalent circuits.

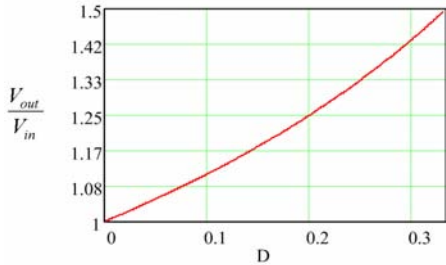


Fig. 5 – Static transfer characteristic in CCM. ( $D < 1/3$ )

**C. Discontinuous Conduction Mode - DCM**

In discontinuous conduction mode, the operational stages are similar to those in CCM, except for the addition of intermediary stages during which no energy is transferred from the input to the load. In other words, the inductor current is equal to zero during a certain amount of time. In this manner, in DCM, the converter presents 9 operational stages which are described below. Fig. 6 presents the main waveforms of the converter for this operational mode.

*1<sup>st</sup> Stage ( $t_0 < t < t_1$ )*

This stage is the same as the first stage in CCM, shown in Fig. 2a. The equivalent circuit of this operational stage is presented in Fig. 4a.

*2<sup>nd</sup> Stage ( $t_1 < t < t_2$ )*

This stage is the same as the second stage in CCM, shown in Fig. 2b. The equivalent circuit of this operational stage is presented in Fig. 4b. This stage ends at  $t_2$  when the current of the input inductor reaches zero and diodes D1, D2, and D3 block naturally.

*3<sup>rd</sup> Stage ( $t_2 < t < t_3$ )*

At  $t_2$ , the current of the input inductor reaches zero. During this stage, the transfer of energy from the input to the load is interrupted and the output capacitor alone supplies the load. This stage ends at  $t_3$  when switch S2 begins conducting. This stage is shown in Fig. 7.

*4<sup>th</sup> Stage ( $t_3 < t < t_4$ )*

This stage is the same as the third stage in CCM, shown in Fig. 2c.

*5<sup>th</sup> Stage ( $t_4 < t < t_5$ )*

This stage is the same as the fourth stage in CCM, shown in Fig. 2b.

*6<sup>th</sup> Stage ( $t_5 < t < t_6$ )*

At  $t_5$ , the current of the input inductor reaches zero, causing diodes D1, D2, and D3 to block naturally. This stage is identical to the third stage and ends at  $t_6$  when switch S3 starts to conduct. This stage is shown in Fig. 7.

*7<sup>th</sup> Stage ( $t_6 < t < t_7$ )*

This stage is similar to the fifth stage in CCM, presented in Fig. 2d.

*8<sup>th</sup> Stage ( $t_7 < t < t_8$ )*

This stage is the same as the sixth stage in CCM, shown in Fig. 2b.

*9<sup>th</sup> Stage ( $t_8 < t < t_9$ )*

At  $t_8$ , the current of the input inductor reaches zero, causing diodes D1, D2, and D3 to block naturally. This stage is the same as the third stage. This stage ends at  $t_9$  when switch S1 begins conducting, thus, initiating a new switching period. This stage is shown in Fig. 7.

**D. Static gain in DCM**

The static characteristic in DCM, parameterized as a function of the load, for different values of parameter  $\gamma$ , is presented in Fig. 8, and is given by:

$$\frac{V_{out}}{V_{in}} = \frac{3 \cdot D^2 + \gamma}{2 \cdot D^2 + \gamma} \tag{5}$$

**E. Output Characteristic**

From analyzing the operation of the converter, the output characteristic of the boost converter operating with  $D < 1/3$  can be determined. Fig. 9 presents the gain of the converter for different duty cycles as a function of  $\gamma$ . Region 1 corresponds to the discontinuous conduction mode, while region 2 corresponds to the continuous conduction mode. It can be observed that the converter using the Y- $\Delta$  cell presents a larger continuous conduction operation area than the classic boost converter and the converter proposed in [1], being this one of the main advantages of the converter proposed by this work when compared to the other two.

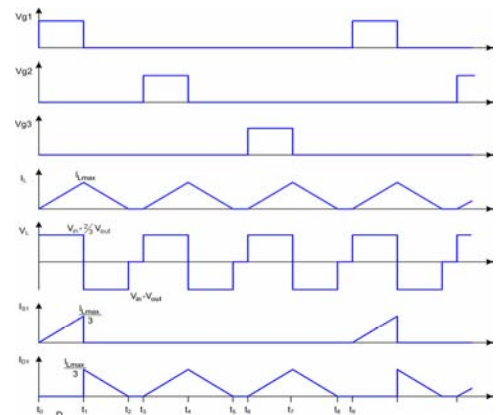


Fig. 6 – Basic waveforms in DCM. ( $D < 1/3$ )

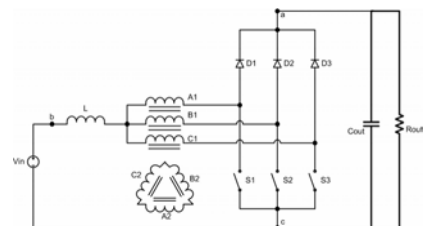


Fig. 7 – Third operating stage in DCM.

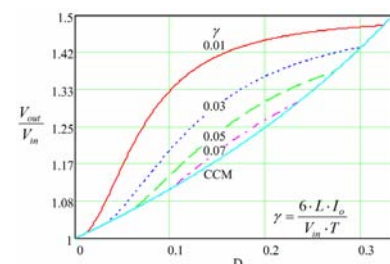


Fig. 8 – Static transfer characteristic in DCM. ( $D < 1/3$ )

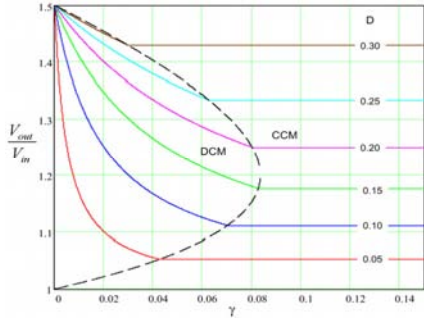


Fig. 9 – Output characteristic of the boost converter. (D<1/3)

F. Inductor ripple current

The input inductor ripple current can be determined by observing the first operating stage, that is, analyzing the voltage across the inductor, given by (1), as well as the duration of the stage. Thus, one obtains:

$$\Delta I_L = \frac{(V_{in} - \frac{2}{3}V_{out}) \cdot D \cdot T}{L} \tag{6}$$

Substituting equation (4) into (6), one obtains:

$$\Delta I_L = D \cdot (1 - 3 \cdot D) \cdot \frac{V_{out}}{3 \cdot L \cdot f} \tag{7}$$

Parameterizing equation (7), equation (8) is obtained, which is depicted in Fig. 10, where the maximum ripple current occurs when the duty-cycle is 1/6, in this case  $\beta$  equals 1/12. Moreover, with a duty-cycle of 1/3 there is no ripple current; therefore, for converters that operate near this point, small inductance values will be necessary in order to obtain a small ripple.

$$\beta = \frac{3 \cdot L \cdot f \cdot \Delta I_L}{V_{out}} = D \cdot (1 - 3 \cdot D) \tag{8}$$

G. Output ripple voltage

The output ripple voltage is a function of the charge provided to the capacitor and its capacitance, as given in (9). Therefore, in order to determine the ripple voltage one should first determine the amount of charge provided to the capacitor, which is given by the integral of the current over time which corresponds to area A1 of Fig. 3, thus, obtaining equation (10).

Substituting (10) into (9) and writing it as a function solely of the output current, equation (11) is obtained:

$$\Delta V = \frac{\Delta Q}{C_{out}} \tag{9}$$

$$\Delta Q = A1 = (I_{in} - I_{out}) \cdot \left(\frac{1}{3} - D\right) \cdot T \tag{10}$$

$$\Delta V = \frac{1}{3} \cdot \frac{I_{out} \cdot (1 - 3 \cdot D) \cdot D}{C_{out} \cdot f \cdot (1 - D)} \tag{11}$$

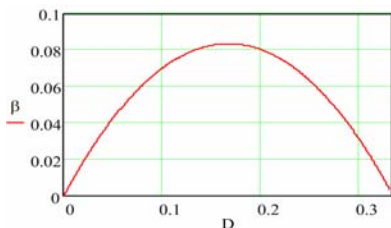


Fig. 10 – Parameterized ripple current. (D<1/3)

H. A study of the transformer

The transformer used is a high-frequency transformer and the windings are placed on a three column core, as shown in Fig. 11. It is important to notice that the transformer doesn't provide isolation and its purpose is to provide a balanced distribution of the currents.

Figure 12 shows the voltage across one of the transformer's windings during a switching period, as well as the current through the winding. Therefore, knowledge of the voltage and the current allows the transformer to be designed.

III. OPERATION WITH 1/3<D<2/3

The operation of the converter with a duty-cycle greater than 1/3 and less than 2/3 is characterized by the superposition of the drive signals of two switches. Therefore, the operating stages will be different from those described previously, when the duty-cycle was less than 1/3.

Next, the main waveforms for the converter operating in CCM and the output characteristic for this operating region will be presented in Fig. 13 and Fig. 14, respectively.

IV. OPERATION WITH 2/3<D<1

The operation of the converter with a duty-cycle greater than 2/3 and less than unity is characterized by the superposition of the drive signals of three switches. Therefore, within this operating region, even in CCM, there will be stages in which no energy will be provided directly from the input to the load, which occurred in other operating regions.

Figure 15 depicts the main waveforms for the converter operating in CCM and Fig. 16 illustrates the output characteristic for this operating region.

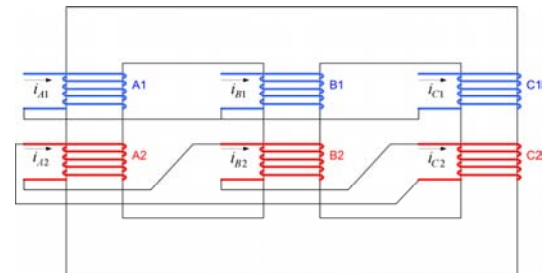


Fig. 11 – Transformer's constructive characteristics.

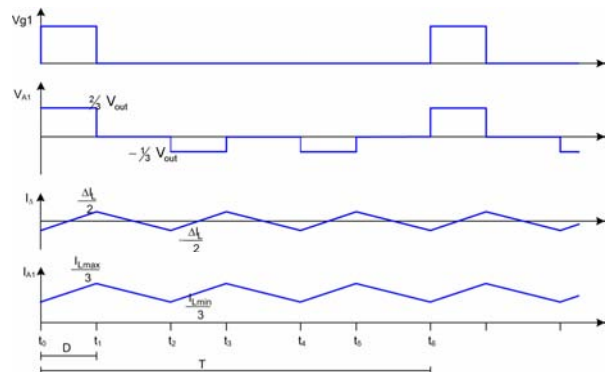


Fig. 12 – Waveforms of the transformer's windings. (D<1/3)

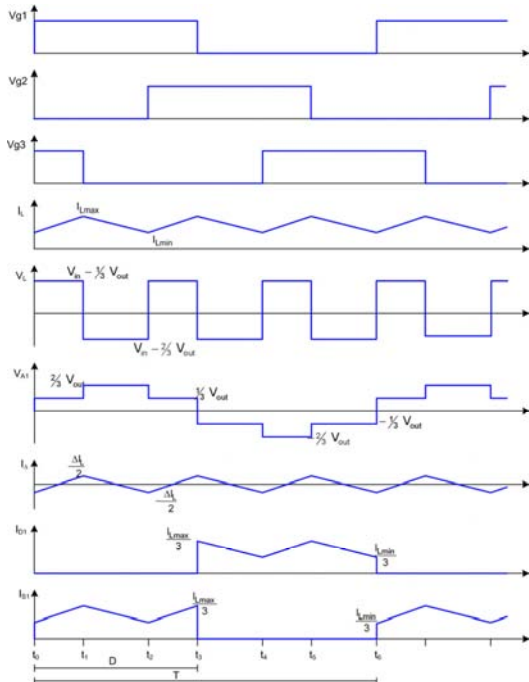


Fig. 13 – Basic waveforms in CCM. ( $1/3 < D < 2/3$ )

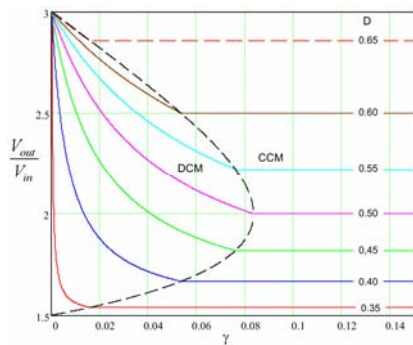


Fig. 14 – Output characteristic. ( $1/3 < D < 2/3$ )

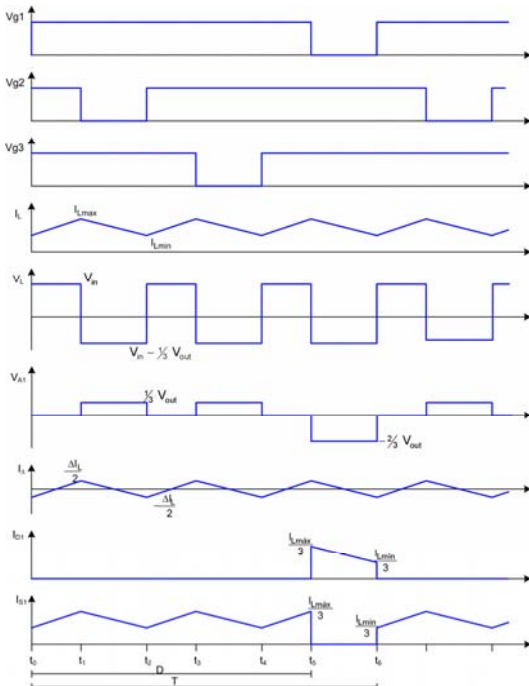


Fig. 15 – Basic waveforms in CCM. ( $2/3 < D < 1$ )

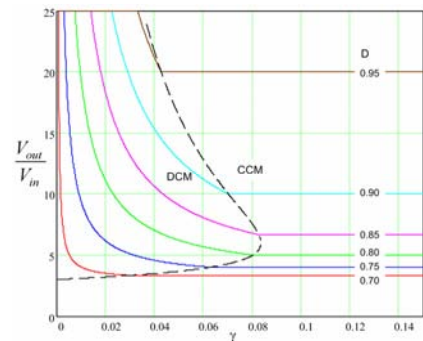


Fig. 16 – Output characteristic. ( $2/3 < D < 1$ )

## V. EXPERIMENTAL RESULTS

In order to demonstrate the principle of operation and validate the analytical studies presented in this paper, a converter with the following characteristics was designed and implemented:

- $P_{out} = 1000$  W, output power;
- $V_{out} = 60$  V, output voltage;
- $V_{in} = 48$  V, input voltage;
- $f = 20$  kHz, switching frequency;
- $L = 10$   $\mu$ H, input inductor;
- $C_{out} = 470$   $\mu$ F, output capacitor.

Figure 17 shows the input current and the output voltage at rated operating conditions, it can be noted that the ripple current is small and its frequency is three times greater than the switching frequency. Figure 18 shows the voltage across a switch and the current through the winding connected to it, it can be noted that the current is approximately 1/3 of the input current.

In Fig. 19 one can observe the voltage and current of the input inductor, however in Fig. 20 the voltage and the current in one of the windings of the transformer are shown.

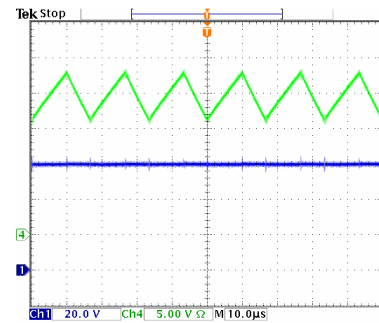


Fig. 17 – Input current and output voltage.

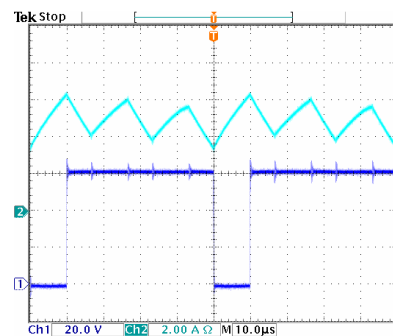


Fig. 18 – Voltage across switch S2 and current through winding B1.

In Fig. 21 the voltage across a switch and the input current when the converter operates with a duty-cycle of  $D=0.33$  are shown; a significant reduction of the input ripple current can be noted here.

In Fig. 22 and Fig. 23 the voltage across a switch and the input current when the converter operates with a duty-cycle of  $D=0.5$  and  $D=0.8$  are shown, respectively.

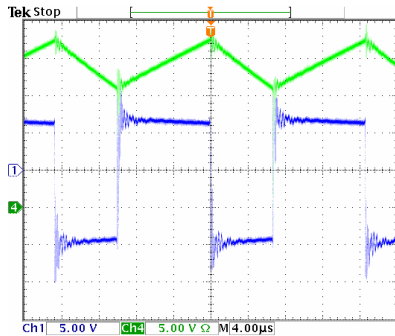


Fig. 19 – Voltage and current of the input inductor.

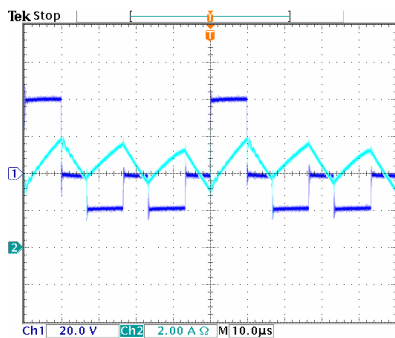


Fig. 20 – Voltage and current of winding B1 of the transformer.

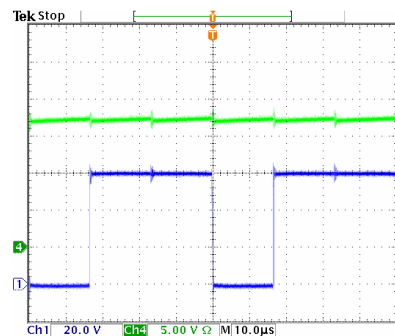


Fig. 21 – Voltage across switch S2 and the input current. ( $D=0.33$ )

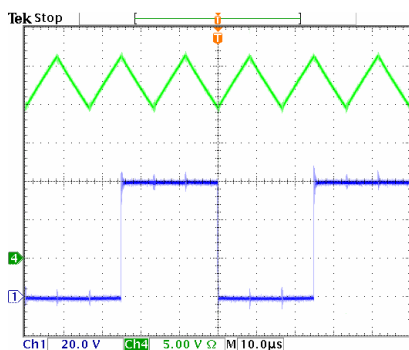


Fig. 22 – Voltage across switch S2 and the input current. ( $D=0.5$ )

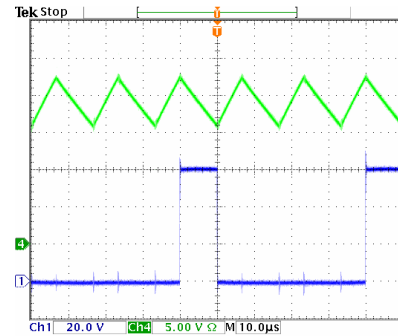


Fig. 23 – Voltage across switch S2 and the input current. ( $D=0.8$ )

## VI. CONCLUSIONS

This article presented a new step-up DC-DC converter based on a commutation cell using a high frequency Y- $\Delta$  transformer. The theoretical analysis of the converter operating with  $D < 1/3$  in both CCM and DCM was performed. The basic waveforms and the output characteristic of the remainder of the regions will be shown.

The proposed converter presents the following advantages: it does not require control circuits to distribute the currents; it reduces the conduction losses of the switches; the frequency of the input and output filters is three times the switching frequency.

The experimental results certify the analysis presented here as well as demonstrate the viability of the converter's usage mainly in low voltage and high current applications.

## ACKNOWLEDGEMENT

We would like to thank the cooperation of Eng. Sérgio V. G. Oliveira for implementing the drive circuit used in this work.

## REFERENCES

- [1] G. T. Bascopé and I. Barbi, "A New Step-Up DC-DC PWM Non-Isolated Converter with a Three-State Commutation Cell" (in Portuguese). CBA 2000 – Brazilian Automation Congress. Florianópolis - September 2000. pp. 778-783.
- [2] S. Kim, "New Multiple DC-DC Converter Topology With a High Frequency Zig-Zag Transformer". Applied Power Electronics Conference and Exposition, 2004. APEC '04. Nineteenth Annual IEEE Volume: 1, 22-26 Feb. 2004. pp. 647 – 653.
- [3] G. T. Bascopé and I. Barbi, "Generation of Family of Non-Isolated DC-DC PWM Converters Using New Three-State Switching Cell". Power Electronics Specialists Conference, 2000. PESC 00. 2000 IEEE 31st Annual ,Volume: 2 , 18-23 June 2000. pp. 858 – 863.
- [4] S. V. G. Oliveira and I. Barbi, "New 3-phase step-up DC-DC converter with 3-phase high frequency transformer". COBEP 2003 - Brazilian Power Electronics Conference. Fortaleza - September 2003. pp. 842-846.